

## Localization at the quenched SU(3) phase transition

---

**Tamas G. Kovacs**<sup>a,b,\*</sup>

<sup>a</sup>*Department of Physics, Eotvos Lorand University,  
Pazmany Peter setany 1/a, 1117 Budapest, Hungary*

<sup>b</sup>*Institute for Nuclear Research,  
Bem ter 18/c, 4026 Debrecen, Hungary*

*E-mail:* [tamas.gyorgy.kovacs@ttk.elte.hu](mailto:tamas.gyorgy.kovacs@ttk.elte.hu)

It is known that the deconfining transition of QCD is accompanied by the appearance of localized eigenmodes at the low end of the Dirac spectrum. In the quenched case localization appears exactly at the critical temperature of deconfinement. In the present work, using quenched simulations exactly at the critical temperature, we show that the localization properties of low Dirac modes change abruptly between the confined and deconfined phase. This means that in the real Polyakov loop sector, the mobility edge has a discontinuity at the critical temperature. In contrast, in the complex sector, there is no such discontinuity at  $T_c$ , even the lowest Dirac modes remain delocalized at the critical temperature in the deconfined phase.

*The 38th International Symposium on Lattice Field Theory, LATTICE2021 26th-30th July, 2021  
Zoom/Gather@Massachusetts Institute of Technology*

---

\*Speaker

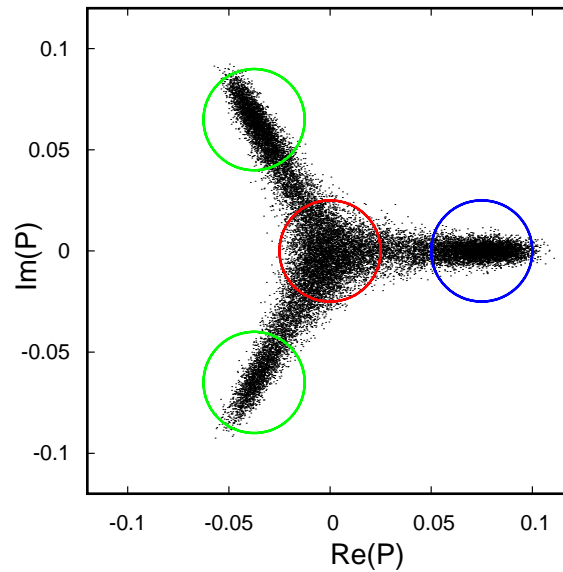


**Figure 1:** Scatter plot of the Polyakov loop in the complex plane. The encircled regions are the different sectors, the confined in the center (red circle), the deconfined real sector on the right (blue circle) and the deconfined complex sectors to the left (green circles).

## 1. Introduction

The spectrum of the QCD Dirac operator is well known to encode many important features of the underlying gauge theory. In particular, it undergoes dramatic changes at the finite temperature transition into the quark-gluon plasma state. In the present work we study how certain properties of the Dirac spectrum change at the finite temperature phase transition of the pure  $SU(3)$  gauge theory. The pure gauge theory provides a good testing ground for this study, since – in contrast to QCD with physical quark masses – this system has a genuine first order phase transition, not just a crossover. As the character of the gluon fields changes dramatically at the phase transition, the corresponding changes in the Dirac spectrum can be easily detected.

The phase transition of the quenched theory is signaled by the spontaneous breaking of the  $Z(3)$  symmetry of the Polyakov loop. While in the low temperature, confining (symmetric) phase the expectation of the Polyakov loop is zero, above the phase transition temperature, in the deconfined phase, the symmetry is spontaneously broken and the Polyakov loop develops a nonzero expectation value, belonging to one of the three  $Z(3)$  sectors. In the present work we perform quenched simulations exactly at the phase transition temperature, where in a finite volume the system can tunnel between the confined and deconfined phase. Therefore, in a simulation performed at the transition temperature we can sample both phases, and in fact, in the deconfined phase all three Polyakov loop sectors as well.

Concerning the Dirac spectrum we have to distinguish three different sectors in terms of the Polyakov loop, and the Dirac spectrum is expected to behave differently in these sectors. These are the confined phase, the real sector in the deconfined phase and the two complex sectors in the

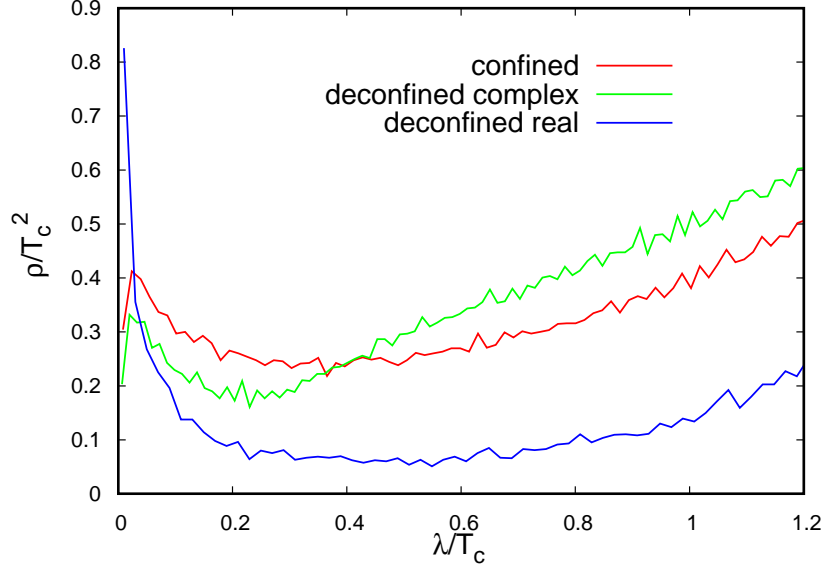


**Figure 2:** The spectral density of the overlap Dirac operator on the three ensembles of  $48^3 \times 8$  lattice configurations at Wilson  $\beta = 6.063$ .

deconfined phase. Due to the complex conjugation symmetry, Dirac spectra in the two complex sectors are the same and we do not have to treat these sectors separately [1]. In Fig. 1 we depict the different sectors by showing a scatter plot of the complex Polyakov loop on an ensemble of  $48^3 \times 8$  lattice configurations exactly at the critical temperature. We can see that although the probability of finding the Polyakov loop in the four above mentioned sectors is enhanced, there is still considerable tunneling among the different sectors.

## 2. Details of the simulation

Let us first summarize the technical details of the simulations. We generated quenched gauge field configurations of spatial linear size  $L = 48$  and temporal size  $N_t = 8$  using the Wilson gauge action at the critical value of the coupling  $\beta = 6.063$ . The configurations were separated into three different groups (sectors) according to the value of the average Polyakov loop. Configurations with  $|P| < 0.03$  were assigned to the confined phase, the ones with  $|P| > 0.06$  were considered to be in the deconfined phase. The latter configurations were further sorted into the real and complex Polyakov loop sector according to the sign of the real part of the Polyakov loop. This set of criteria was found to include the peaks of the Polyakov loop distribution into the respective sectors (see Fig. 1). We computed the lowest 100 eigenvalues (with positive imaginary parts) of the overlap Dirac operator separately on the three ensembles of configurations belonging to the above three sectors.

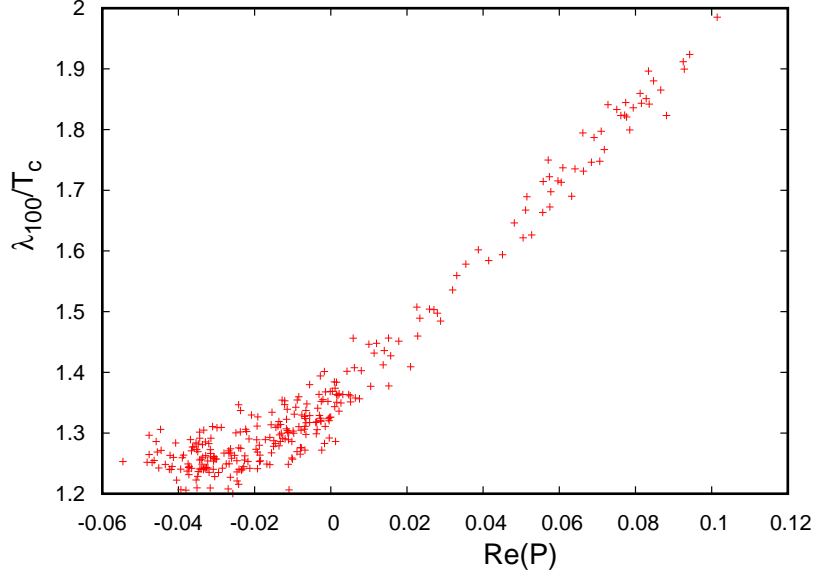


**Figure 3:** Scatter plot of the real part of the average Polyakov loop versus the  $100^{\text{th}}$  smallest Dirac eigenvalue on a set of lattice configurations.

### 3. Results

The simplest quantity characterizing the Dirac spectrum is the spectral density. In Fig. 2 we compare the spectral density in the three different sectors. The confined phase and the deconfined complex sectors exhibit qualitatively similar spectral densities. In contrast, the spectral density in the deconfined real sector is markedly different. It has a high, but narrow spike at the very low end, above which the spectral density drops considerably. The narrow spike in the spectral density can be attributed to mixing instanton-antiinstanton zero modes that produce several pairs of complex eigenvalues of rather small magnitude [2]. Although in the other two sectors there is also a slight accumulation of eigenvalues near zero, this is by far less pronounced than in the real sector. This is caused by a stronger mixing of topological zero modes, which in the confined phase is due to a higher density of topological fluctuations. In the deconfined complex Polyakov sectors this stronger mixing can be attributed to the more extended nature of the topological zero modes [3]-[5].

The difference in the bulk spectral density between the real and complex sector in the confined phase can be qualitatively understood by considering the lowest Matsubara modes in the free theory with different boundary conditions. Indeed, the effective boundary condition for the Dirac equation is a combination of the phase  $\pi$ , coming from the antiperiodic boundary condition for fermions, and the phase of the Polyakov loop. In the real sector the Polyakov loop phase is zero, in the complex sectors, it is  $\pm 2\pi/3$ , making the magnitude of the overall effective phase  $\pi$  and  $\pi/3$ , respectively. Thus the lowest free Matsubara mode is much higher in the real sector, and this makes the density of low-lying bulk modes considerably lower also in the interacting case. In fact, this is how the breaking of the  $Z(3)$  symmetry by dynamical quarks can be understood, since the quark determinant favors the real sector that has fewer small eigenvalues.

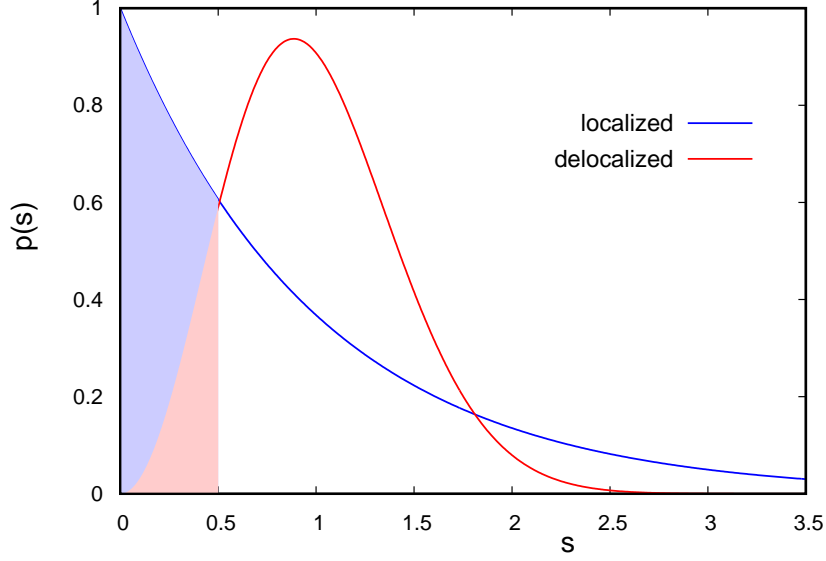


**Figure 4:** The unfolded level spacing distribution, corresponding to localized and delocalized modes. The red shaded region depicts the integral, defining  $I_{0.5}$  for the delocalized case, the blue one the difference of the integrals for the localized and the delocalized case.

The direct connection between the Polyakov loop and the Dirac spectrum is further demonstrated in Fig. 3, where we plot the real part of the average Polyakov loop versus the  $100^{th}$  eigenvalue of the Dirac operator. For positive real part there is a strong correlation between the two quantities. It is clear that the more ordered the Polyakov loop is in the real sector, the fewer low eigenvalues the Dirac operator has.

#### 4. Localization at $T_c$

It is known that in the high temperature phase the lowest part of the Dirac spectrum consists of localized eigenmodes (for a recent review see [6]). Approaching the transition temperature from above, the mobility edge, separating the low localized modes from the bulk of the spectrum, moves toward zero, and when it reaches zero, all modes become delocalized, as expected in the low temperature phase. In the quenched case, by extrapolating the mobility edge, it was found to vanish exactly at the critical temperature [7, 8]. A naturally arising question is whether the lowest part of the spectrum is localized or delocalized exactly at the critical point. More precisely, the extrapolations presented in Refs. [7, 8] are compatible both with a continuously vanishing mobility edge and one that has a discontinuity at the phase transition. Our present simulation, done exactly at the critical point, gives us an opportunity to distinguish these two possibilities. This can be done by looking at the localization properties of the lowest Dirac modes separately in the confining and the deconfining phase and comparing the values of the mobility edge in the two phases.

The simplest way to decide whether eigenmodes in a certain region of the spectrum are localized or delocalized is to compute the unfolded level spacing distribution (ULSD). If the modes

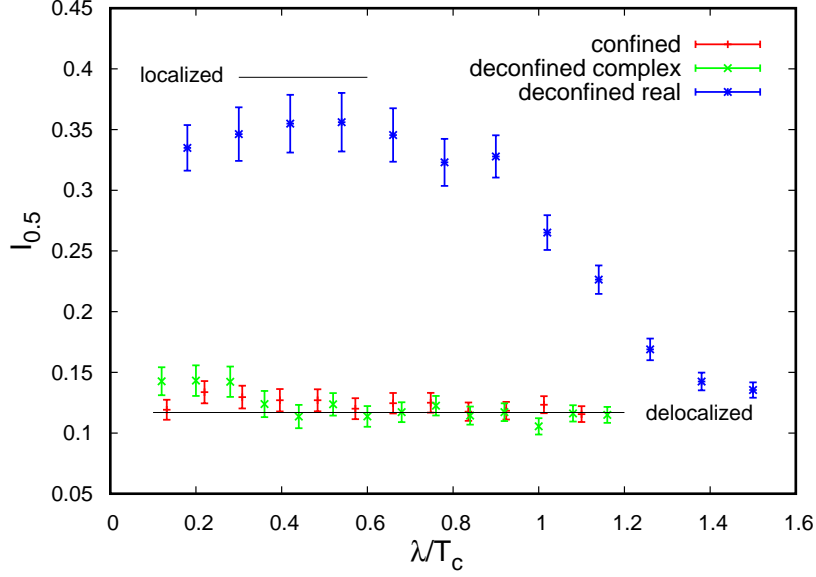


**Figure 5:** The parameter  $I_{0.5}$  across the spectrum computed separately in the three different sectors, the confined phase and in the deconfined phase in the real and the complex sector on the  $48^3 \times 8$  lattices.

are localized, the corresponding eigenvalues are statistically independent, they are described by a Poisson distribution, and the unfolded level spacing distribution is exponential. If the eigenmodes are delocalized, the ULSD is well approximated by the Wigner surmise of the corresponding random matrix universality class, which in the case of the overlap Dirac operator, is the unitary class. In Fig. 4 these two distributions are shown. A convenient way to monitor how the distribution changes across the spectrum is to consider instead of the whole distribution, just a single parameter that can distinguish the two extreme cases (localized and delocalized). For this purpose we use the parameter

$$I_{0.5} = \int_0^{0.5} p(x) dx, \quad (1)$$

where the upper limit of the integration was chosen to be the crossing point of the two distributions (approximately 0.5) to maximize the difference between the two limiting cases (see Fig. 4).

To monitor how the ULSD changes across the spectrum and to determine the mobility edge, we split the spectrum into narrow bins and in each bin separately compute the parameter  $I_{0.5}$ . For details of the unfolding and how we assign the eigenvalue pairs to bins, see the Appendix of Ref. [8]. We repeated this procedure for all three sectors, i.e. the confined phase and for the deconfined phase in the real and complex sector. The results are shown in Fig. 5. It is clear from the figure that both in the confined phase and in the deconfined complex sector, already the lowest Dirac modes are delocalized, thus the mobility edge is effectively at zero. However, in the deconfined real sector, in the one that would be selected if dynamical fermions were present, there is a finite range in the spectrum above zero where the eigenmodes seem to be localized. In this region  $I_{0.5}$  almost reaches the value expected for localized modes. The slight deviation might be due to the finite system size or some more subtle effects (see Refs. [9]-[11]). Notwithstanding these details, it is obvious from the

figure that the localization properties of the lowest Dirac eigenmodes change abruptly between the confined phase and the deconfined real Polyakov sector (the physical sector). This is consistent with the fact that the transition in the  $SU(3)$  pure gauge theory is first order. It is, however, surprising that the deconfined complex Polyakov sector does not exhibit such an abrupt change, the lowest modes there are delocalized, like in the confined phase.

## 5. Conclusions

In the present paper we studied how the spectral properties of the Dirac operator change at the finite temperature first order phase transition of the pure  $SU(3)$  gauge theory. We showed that the phase transition is accompanied by discontinuous changes in the spectral properties. Namely, both the spectral density around zero and the localization properties of the lowest modes change abruptly at the transition. In particular, there is a band around zero in the spectrum, where the corresponding eigenmodes become localized at the transition in the real Polyakov loop sector. This also implies that the mobility edge is discontinuous at the transition if we restrict our attention to the real (physical) Polyakov loop sector. In contrast, in the complex sector even the lowest eigenmodes remain delocalized at the transition. This property can be qualitatively understood by the more extended nature in this sector of zero modes carried by Kraan-van Baal calorons.

## References

- [1] M. Cardinali, M. D’Elia, F. Garosi and M. Giordano, *Localization properties of Dirac modes at the Roberge-Weiss phase transition* [arXiv:2110.10029 [hep-lat]].
- [2] R. A. Vig and T. G. Kovacs, *Ideal topological gas in the high temperature phase of  $SU(3)$  gauge theory*, Phys. Rev. D **103**, no.11, 114510 (2021) doi:10.1103/PhysRevD.103.114510 [arXiv:2101.01498 [hep-lat]].
- [3] T. C. Kraan and P. van Baal, *Periodic instantons with nontrivial holonomy*, Nucl. Phys. B **533**, 627-659 (1998) doi:10.1016/S0550-3213(98)00590-2 [arXiv:hep-th/9805168 [hep-th]].
- [4] C. Gattringer, M. Gockeler, P. E. L. Rakow, S. Schaefer and A. Schaefer, *A Comprehensive picture of topological excitations in finite temperature lattice QCD*, Nucl. Phys. B **618**, 205-240 (2001) doi:10.1016/S0550-3213(01)00509-0 [arXiv:hep-lat/0105023 [hep-lat]].
- [5] C. Gattringer and S. Schaefer, *New findings for topological excitations in  $SU(3)$  lattice gauge theory*, Nucl. Phys. B **654**, 30-60 (2003) doi:10.1016/S0550-3213(03)00083-X [arXiv:hep-lat/0212029 [hep-lat]].
- [6] M. Giordano and T. G. Kovacs, *Localization of Dirac Fermions in Finite-Temperature Gauge Theory*, Universe **7**, no.6, 194 (2021) doi:10.3390/universe7060194 [arXiv:2104.14388 [hep-lat]].
- [7] T. G. Kovacs and R. A. Vig, *Localization transition in  $SU(3)$  gauge theory*, Phys. Rev. D **97**, no.1, 014502 (2018) doi:10.1103/PhysRevD.97.014502 [arXiv:1706.03562 [hep-lat]].

- 
- [8] R. A. Vig and T. G. Kovacs, *Localization with overlap fermions*, Phys. Rev. D **101**, no.9, 094511 (2020) doi:10.1103/PhysRevD.101.094511 [arXiv:2001.06872 [hep-lat]].
- [9] A. Alexandru and I. Horváth, *Possible New Phase of Thermal QCD*, Phys. Rev. D **100**, no.9, 094507 (2019) doi:10.1103/PhysRevD.100.094507 [arXiv:1906.08047 [hep-lat]].
- [10] A. Alexandru and I. Horváth, *Unusual Features of QCD Low-Energy Modes in the Infrared Phase*, Phys. Rev. Lett. **127**, no.5, 052303 (2021) doi:10.1103/PhysRevLett.127.052303 [arXiv:2103.05607 [hep-lat]].
- [11] A. Alexandru and I. Horváth, *Anderson Metal-to-Critical Transition in QCD*, [arXiv:2110.04833 [hep-lat]].